The Journal of Neuroscience, August 15, 2002, 22(16):7206–7217

Genetic Influence on Quantitative Features of Neocortical Architecture

Matthias Kaschube,[1,2]* Fred Wolf,[1,3]* Theo Geisel,[1] and Siegrid Löwel[2]

[1]Max-Planck-Institut für Strömungsforschung and Fakultät für Physik, Universität Göttingen, 37073 Göttingen, Germany, [2]Forschergruppe "Visuelle Entwicklung und Plastizität," Leibniz–Institut für Neurobiologie, 39118 Magdeburg, Germany, and [3]Institute for Theoretical Physics, University of California, Santa Barbara, California 93106

The layout of functional cortical maps exhibits a high degree of interindividual variability that may account for individual differences in sensory and cognitive abilities. By quantitatively assessing the interindividual variability of orientation preference columns in the primary visual cortex, we demonstrate that column sizes and shapes as well as a measure of the homogeneity of column sizes across the visual cortex are significantly clustered in genetically related animals and in the two hemispheres of individual brains. Taking the developmental timetable of column formation into account, our data indicate a substantial genetic influence on the developmental specification of visual cortical architecture and suggest ways in which genetic information may influence an individual's visual abilities.

Key words: visual cortex; development; orientation columns; cortical maps; area 17; genetic determination

In most areas of the cerebral cortex, information is processed in two-dimensional (2D) arrays of functional modules, called cortical columns (LeVay and Nelson, 1991; Creutzfeldt, 1995). Neurons in individual columns are densely connected by local intracortical circuits and share many functional properties (e.g., stimulus selectivities in sensory cortical areas or movement specificities in motor cortical areas). In a plane parallel to the cortical surface, neuronal selectivities vary systematically, so that columns of similar functional properties form highly organized 2D patterns, known as functional cortical maps. This 2D organization of a cortical area appears closely related to its intrinsic circuitry and computational capabilities: the organization of intracortical synaptic connections is tightly matched to the exact spatial arrangement of functional columns (Somogyi et al., 1998), and improvements of both sensory and motor performance have repeatedly been linked to learning-induced plasticity of column arrangements (Recanzone, 2000). Many lines of evidence suggest that during the ontogenetic development of the cerebral cortex, functional maps typically form through activity-dependent refinement of initially crude patterns of synaptic connections (Stryker, 1991; Goodman and Shatz, 1993; Singer, 1995; Price and Willshaw, 2000). Therefore, epigenetic factors such as spontaneously generated patterns of neuronal activity (Weliky and Katz, 1999) or individual experience (Blakemore and Cooper, 1970; Singer et al., 1981; Frégnac and Imbert, 1984; Sengpiel et al., 1999) are widely believed to play a decisive role in specifying the precise layout of functional cortical maps. Recently, however, a series of experiments indicated that the initial development of these maps is much less dependent on experience than previously thought (Gödecke and Bonhoeffer, 1996; Crair et al., 1998; Löwel et al., 1998; Crowley and Katz, 2000) and raised the urgency of exploring the largely unknown role of genetic information in functional cortical development.

To explore the impact of genetic factors on cortical architecture, we therefore analyzed the variability of patterns of orientation preference columns [OR columns, columns of neurons preferentially responding to visual contours of a particular orientation (Hubel and Wiesel, 1962)] in the primary visual cortex in genetically related and unrelated animals raised in the same visual environment. Using this approach, a strong impact of genetic factors should show up as a reduced variability (i.e., enhanced similarity of column patterns in genetically related animals compared with the overall interindividual variability within the population). To test for such a reduced variability of column patterns, we used a newly developed image analysis technique to quantify the basic properties of the layout of orientation columns in the primary visual cortex. These analyses revealed that (1) the sizes and shapes of visual cortical orientation columns exhibit a high degree of interindividual variability, and (2) column sizes and shapes as well as a measure of the homogeneity of column sizes across the visual cortex are significantly clustered in genetically related animals and in the two hemispheres of individual brains. Taking the developmental timetable of column formation into account, these observations indicate a substantial genetic influence on the developmental specification of visual cortical architecture.

MATERIALS AND METHODS

Animals. We analyzed 2-deoxyglucose (2-DG)-labeled patterns of OR columns in the primary visual cortex (area 17) of 31 adult cats (48 hemispheres). OR maps of these animals have been previously published (Löwel et al., 1987, 1988; Löwel and Singer, 1990). Table 1 lists details of the dataset used in the present analysis. To assess littermate clustering, data from 22 cats born and raised in the same overall visual environment, namely the animal house of the Max-Planck-Institut für Hirnforschung (Frankfurt am Main, Germany), were used. The nursing facilities con-

Received March 5, 2002; revised May 6, 2002; accepted May 15, 2002.

This work was supported by the Wissenschaftsgemeinschaft Gottfried Wilhelm Leibniz, The National Science Foundation, and the Max-Planck-Gesellschaft. We thank Wolf Singer for permission to use the 2-DG autoradiographs obtained by S.L. in his laboratory for quantitative analysis. We also thank John M. Crook and Thomas Dresbach for valuable comments on a previous version of this manuscript and Steffi Bachmann for excellent technical assistance.

*M.K. and F.W. contributed equally to this work.

Correspondence should be addressed to Dr. Fred Wolf, Department of Nonlinear Dynamics, Max-Planck-Institut für Strömungsforschung, Bunsenstrasse 10, 37073 Göttingen, Germany. E-mail: fred@chaos.gwdg.de.

 0270-6474/02/227206-12$15.00/0

Table 1. Dataset used for quantitative analysis of OR maps in cat area 17

Animal	Hemispheres	Autoradiographs	Stimulus	Age (weeks)
C1-L1	Le+Ri	4/4	0°	9.5
C2-L1	Le+Ri	5/2	0°	10
C3-L1	Le+Ri	4/4	0°	8
C4-L2	Le+Ri	3/4	0°	7.5
C5-L2	Le+Ri	5/6	90°	8
C6-L3	Le+Ri	5/5	90°	8
C7-L3	Le+Ri	4/4	0°	8
C8-L4	Le+Ri	4/4	90°	14.5
C9-L4	Ri	4	90°	14.5
C10-L5	Ri	5	0°	12
C11-L5	Ri	4	0°	12
C12-L6	Ri	4	90°	13
C13-L6	Ri	3	90°	13
C14	Le+Ri	4/4	90°	10
C15	Le+Ri	4/4	90°	8
C16	Le+Ri	4/4	90°	12
C17	Le+Ri	4/4	0°	6
C18	Le+Ri	5/5	45°	7
C19	Le	4	0°	9.5
C20	Ri	4	90°	10
C21	Le	4	45°	21
C22	Ri	4	0°	8
C23	Le+Ri	4/3	135°/0°	13
C24	Le+Ri	4/4	135°/0°	8
C25	Le+Ri	4/4	0°	10
C26	Le+Ri	4/4	0°	9
C27	Ri	4	0°	10.5
C28	Le	4	0°	13
C29	Ri	3	90°	12
C30	Ri	5	90°	12
C31	Ri	3	90°	12

We analyzed a total of 48 hemispheres from 31 animals (C1–C31), including six litters (L1–L6). Animals belonging to the same litter are labeled accordingly. Litter 1 (L1) consisted of three animals (C1–L1, C2–L1, and C3–L1); litters 2–6 (L2–L6) consisted of two animals. For every animal, the table lists the hemispheres (Le, left; Ri, right; Le+Ri, both), the number of 2-DG autoradiographs analyzed, the orientation of the visual stimulus (0° = horizontal, 90° = vertical, 45° = right oblique, and 135° = left oblique), and the age at the time of the experiment. All littermates and cats C14–C22 were born and raised in the animal house of the Max-Planck-Institut für Hirnforschung (Frankfurt am Main, Germany). Animals C23–C31 were bought from the professional animal breeding companies Ivanovas (C23–C28) and Gaukler (C29–C31), both in Germany.

sisted of two nearly identical rooms with bar cages and tiled floors and walls. At all times, the crew of the animal house cared for all animals, so that no particular person was assigned to only a subset of the animals. Each room contained up to 18 cages, so that animals had visual and other social contact not only with their littermates and mothers but with all of the other animals living in the same room as well. All animals in the colony were mongrels. For impregnation, female cats were given the opportunity to mate with 2-3 tomcats. Tomcats in the colony were exchanged regularly. All litters in the sample used in this study were born and raised by different mothers.

All animals stayed in these rooms until the 2-DG experiments. The 2-DG experiments were performed between January 31, 1984 and August 25, 1987 by the same main experimenter (S. Löwel) in the same laboratory, keeping the visual experience of all animals very similar. The visual stimuli during the 2-DG experiments were always identical in spatial and temporal frequency and only differed in orientation, whereby orientation presentation within the two groups (littermates vs nonlittermates) was rather balanced (see Table 1): in the littermates, horizontal contours (0°) were used in 57% of cases (12 of 21), and vertical contours (90°) were used in 43% of cases (9 of 21); in nonlittermates, 0° were used in 44% of cases (12 of 27), 90° were used in 37% of cases (10 of 27), 45° were used in 11% of cases (3 of 27), and 135° were used in 7% of cases (2 of 27). The 22 animals raised in Frankfurt included six litters (one litter of three siblings and five litters of two siblings). In addition, data from another nine animals, bought from two animal breeding companies in Germany (Ivanovas, Kisslegg im Allgäu, Germany; Gaukler, Offenbach, Germany), were used for the assessment of the overall variability of parameter values, for the calculation of correlations among various parameters, and for the calculation of correlations of left and right hemisphere parameter values.

Image digitization. Photoprints of the 2-DG autoradiographs were digitized using a flat-bed scanner (OPAL ultra; Linotype-Hell AG, Eschborn, Germany, operated using Corel Photoshop; Corel, Ottawa, Ontario, Canada) with an effective spatial resolution of 9.45 pixels/mm cortex and 256 gray levels per pixel. For every autoradiograph, this yielded an array of gray values $I_0(x)$, where x is the position within the area and I_0 its intensity of labeling.

Region of interest. For every autoradiograph, a region of interest encompassing the pattern labeled in area 17 was defined by visual inspection. The 17/18 border was identified based on the larger column spacing and different pattern layout in area 18 compared with area 17 (Löwel et al., 1987). The manually defined polygon encompassing the entire 2-DG pattern within area 17 was stored together with every autoradiograph. Only the pattern within area 17 was used for subsequent analysis. Regions including artifacts (scratches, folds, and air bubbles) were excluded from further analysis.

Preprocessing. The digitized patterns were preprocessed to remove overall variations in the intensity of labeling. To achieve this, the local average labeling intensity:

$$\bar{I}(x) = \int_{A17} d^2y I_0(y) K(y-x) \Big/ \int_{A17} d^2y K(y-x), \quad (1)$$

was calculated using the kernel $K(y) = \frac{1}{2\pi\sigma_x^2} \exp(-y^2/2\sigma_x^2)$ and subtracted from the pattern:

$$I_1(x) = I_0(x) - \bar{I}(x). \quad (2)$$

The spatial width σ_x of the kernel was determined from the requirement that structures with a wavelength of <1.5 mm, the range of column sizes, should not be strongly attenuated by the preprocessing. We used $\sigma_x = 0.43$ mm, for which the attenuation at wavelengths of <1.5 mm is <20%. This choice was sufficient to remove overall variations in labeling intensity but left the column pattern unaffected in all autoradiographs. The pattern $I_1(x)$ was then centered and normalized by subtracting its average gray value and dividing by the SD of gray values, resulting in an array $I(x)$ with:

$$0 = \int_{A17} d^2y\, I(y), \quad (3)$$

$$1 = \int_{A17} d^2y (I(y))^2 \Big/ \int_{A17} d^2y. \quad (4)$$

Finally, in artifact regions and regions outside of area 17, the gray values of the patterns were set to zero. Figure 1 shows representative examples of original and preprocessed patterns.

Analysis of column layout. For every autoradiograph, 2D maps of local column spacing and of a measure of domain anisotropy or bandedness were estimated based on wavelet transforms (Farge, 1992) of $I(x)$:

$$\hat{I}(x,\theta,l) = \int_{A17} d^2y I(y)\, \psi_{x,\theta,l}(y). \quad (5)$$

Here x, θ, l are the position, orientation, and scale of the wavelet $\psi_{x,\theta,l}(y)$, and $\hat{I}(x, \theta, l)$ denotes the array of wavelet coefficients. We used complex-valued Morlet-wavelets defined by a mother wavelet:

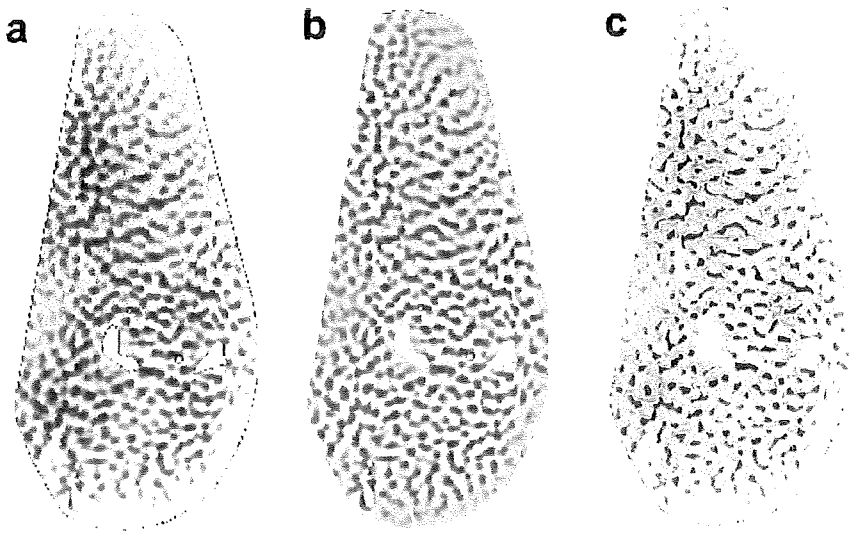

Figure 1. Preprocessing leaves the essential spatial properties of the 2-DG patterns unaffected. *a*, Typical 2-DG pattern. *b*, Preprocessed 2-DG pattern. *c*, The zero contours of the preprocessed 2-DG pattern (*yellow lines*) are superimposed on the original autoradiograph in *a*. Note that the zero contours closely follow the *outlines* of the labeled domains.

$$\psi(x) = \exp\left(-\frac{1}{2}x^T\begin{pmatrix}1 & 0\\ 0 & \sigma_y^{-2}\end{pmatrix}x\right)e^{ik_\psi x}, \tag{6}$$

and

$$\psi_{x,\theta,l}(y)=l^{-1}\psi\left(\Omega^{-1}(\theta)\frac{y-x}{l}\right), \tag{7}$$

with the rotation matrix $\Omega(\theta)=\begin{pmatrix}\cos(\theta) & -\sin(\theta)\\ \sin(\theta) & \cos(\theta)\end{pmatrix}$. The characteristic wavelength of a wavelet with scale l is $\Lambda_\psi l$ with $\Lambda_\psi = 2\pi/|k_\psi|$. For large values of $|k_\psi|$, the wavelets in Equation 6 exhibit a high resolution of spatial frequencies. For small values of $|k_\psi|$, they are localized in the cortical coordinates enabling high spatial resolution. The parameter σ_y determines the degree of anisotropy of the wavelets, with larger values leading to a higher sensitivity for elongated, bandlike structures. Therefore we used large $|k_\psi|$ wavelets of moderate anisotropy ($k_\psi = (7, 0)$, $\sigma_y = 1$) to estimate the column spacing and small $|k_\psi|$ wavelets of enhanced anisotropy ($k_\psi = (2, 0)$, $\sigma_y = 1.5$) to calculate the local anisotropy parameter. With these choices, patterns with large or small columns and with patchy or bandlike appearance were well discriminated by the measures described in the following paragraphs.

Spacing. The orientation averaged modulus:

$$\bar{I}(x,l) = \int_0^\pi \frac{d\theta}{\pi}|\hat{I}(x,\theta,l)|, \tag{8}$$

of the wavelet coefficients was used to estimate the local column spacing. For every position x, the scale:

$$\bar{l}(x) = argmax(\bar{I}(x,l)), \tag{9}$$

maximizing $\bar{I}(x, l)$ was determined. The corresponding characteristic wavelength:

$$\Lambda(x) = \bar{l}(x)\Lambda_\psi, \tag{10}$$

was used as an estimate for the local column spacing at the position x. For every position (spatial grid size, 0.11 mm), wavelet coefficients for six orientations $\theta_i \in \{0, \pi/6, \ldots, 5\pi/6\}$ and 12 scales l_j (with $l_j\Lambda_\psi$ equally spaced in 0.5 mm, 2 mm) were calculated. The scale maximizing $\bar{I}(x, l)$ was then estimated as the maximum of a polynomial in l fitting the $[\bar{I}(x, l_j)]$ for a given position x (least square fit).

Bandedness. The orientation dependence of the wavelet coefficients was used to calculate a parameter measuring the anisotropy of local pattern elements (Fig. 2). For a pattern consisting of isotropic patches, the wavelet coefficients depend only weakly on the orientation θ of the wavelet. For a pattern consisting of elongated bands, the magnitude of the wavelet coefficients depends strongly on wavelet orientation and is largest if the orientation of the wavelet matches the orientation of the bands. Using only coefficients at the local wavelength $\Lambda(x)$, we therefore calculated:

$$s'(x) = \int_0^\pi d\theta|\hat{I}(x,\theta)|^2e^{i2\theta}\Big/\int_0^\pi d\theta|\hat{I}(x,\theta)|^2, \tag{11}$$

and used the modulus $|s(x)|$ of the local average of this quantity:

$$s(x) = \int_{A17} d^2x's'(x')K(x'-x)\Big/\int_{A17} d^2x'K(x'-x), \tag{12}$$

with $K(x) = \frac{1}{2\pi\sigma^2}\exp(-\frac{x^2}{2\sigma^2})$ and $\sigma = 1.3 <\Lambda(x)>_x$ as a local measure of bandedness. Here $<\Lambda(x)>_x$ is the average local wavelength. Here and in the following, $\langle\cdot\rangle_x$ denotes averaging over all locations in area 17. With this choice of σ, $s(x)$ is sensitive to the occurrence of bandlike regions that extend at least over the size of a hypercolumn. Wavelet coefficients for the scale corresponding to the local column spacing and for nine orientations $\theta_i \in \{0, \pi/9, \ldots, 8\pi/9\}$ were calculated for every position and used to evaluate Equations 11 and 12. Based on the local column spacing, $\Lambda(x)$, and the local bandedness, $|s(x)|$, the overall layout of the 2-DG patterns was characterized by four parameters: mean column spacing, $\Lambda = \Lambda(x)_x$; the SD of local column spacing across area 17, $\sigma_\Lambda = \sqrt{\langle(\Lambda(x) - \Lambda)^2\rangle_x}$, called spacing inhomogeneity in the following; mean bandedness, $\alpha = \langle|s(x)|\rangle_x$; and the SD of the local anisotropy parameter, $\sigma_\alpha = \sqrt{\langle(|s(x)| - \alpha)^2\rangle_x}$, called shape inhomogeneity in the following.

Accuracy of parameter estimation. To estimate these parameters reliably and precisely, up to six autoradiographs derived from flat-mount sections at various cortical depths were analyzed for every brain hemisphere. The parameter values for the spacing parameters Λ and σ_Λ were estimated with an average SE of <20 μm (Table 2). The dimensionless shape parameters α and σ_α, which range between 0.06 and 0.3, were estimated with an average SE of <0.01 (Table 2). Qualitatively and quantitatively the results reported were insensitive to variation of the parameters of the image analysis method such as σ, σ_x, k_ϕ, and the number of used wavelet orientations and scales.

Permutation tests. Because the distributions of parameter values were not Gaussian, permutation tests were used to assess the statistical significance of littermate clustering, correlations of parameter values of left and right hemispheres, and correlations between parameters. The approach can be summarized as follows: To assess whether parameter values in littermates were significantly clustered, we compared the similarity of parameter values among real littermates with the similarity of parameter values found in randomly chosen sets of animals raised in the

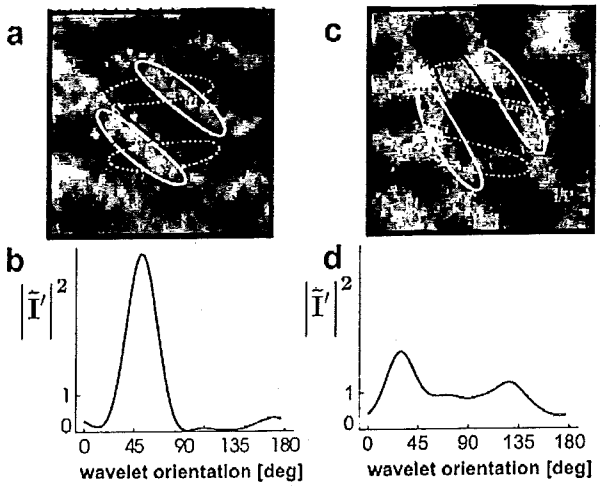

Figure 2. Analyzing the shape of orientation columns. *a*, Examples of wavelets $\psi_{\theta,x}$ with different orientation θ superimposed on a stripe-like region of 2-DG-labeled orientation columns. The real parts of the complex-valued wavelets are shown. Positive regions are delineated by *white lines*; negative regions are delineated by *dark lines*. The wavelet of optimal orientation (*solid lines*) and one example of nonoptimal orientation (*dotted lines*) are shown. *b*, The normalized squared modulus of the wavelet coefficients:

$$|\tilde{I}'(\theta,x)|^2 = |\tilde{I}(\theta,x)|^2 \Big/ \int_0^{180} |\tilde{I}(\theta,x)|^2 \frac{d\theta}{180},$$

as a function of orientation θ. For a vertically oriented wavelet, $\theta = 0°$, 180°. *c*, Wavelets $\psi_{\theta,x}$ superimposed on a patchy region of 2-DG-labeled orientation columns and the respective coefficients (*d*) (description as in *a* and *b*). Note that for the stripe-like region, $|\tilde{I}|^2$ is strongly modulated and exhibits a pronounced peak at the wavelet orientation θ matching the stripe orientation. This is not the case for the patchy region.

same environment. Statistically, there is significant littermate clustering if the hypothesis: "Parameter values are independent of an animals' genetic identity" is rejected (i.e., if the observed degree of similarity is extremely unlikely to occur by chance). To test this hypothesis, we calculated a single number [the average distance to the litter mean (ADLM), see below] that quantifies the similarity of parameter values among littermates and compared its actual value with the statistical distribution predicted by the hypothesis that the parameter values are independent of an animal's genetic identity.

P values were calculated using 10^6 randomly generated permutations of the data. For the analysis of littermate clustering, we calculated the ADLM ΔQ for parameter $Q \in \{\Lambda, \sigma_\Lambda, \alpha, \sigma_\alpha\}$ according to:

$$\Delta Q = \sum_i |Q_i - \bar{Q}_{l(i)}|/N, \tag{13}$$

where i indexes hemispheres, $l(i)$ is the index of the litter to which hemisphere i belongs, $\bar{Q}_{l(i)}$ is the average of parameter values within this litter, and N is the total number of hemispheres in all litters. Small values of ΔQ indicate littermate clustering. If parameter values in genetically related animals or hemispheres are statistically independent (i.e., genetic information plays no role in the specification of parameter Q), the probability to observe an ADLM as small as or smaller than ΔQ is:

$$P = \langle \Theta(\Delta Q - \Delta Q_p) \rangle_p, \tag{14}$$

where $\Delta Q_p = \Sigma_i |Q_{p(i)} - \bar{Q}_{l(p(i))}|/N$ is the ADLM of pseudolitters generated by a suitable permutation $p(i)$ of hemisphere indices, $\Theta(\bullet)$ is the Heaviside function, and $\langle \bullet \rangle_p$ denotes the average over permutations. *p* values were calculated using either arbitrary random permutation (P_{II}) or only such permutations that preserved left–right pairs of hemisphere indices (P_I). Histograms of ΔQ_p values for these two randomization schemes are displayed in Figure 10i–l. *P* values for correlation coefficients were calculated analogous to the calculation of P_{II} values.

RESULTS

Using a newly developed technique based on wavelet analysis, we quantified the major layout properties of OR column patterns obtained by 2-DG autoradiography in the cat primary visual cortex (area 17) (Löwel et al., 1987, 1988; Löwel and Singer, 1990; Kaschube et al., 2000). In all investigated hemispheres (48 hemispheres from 31 animals), OR columns preferring the same stimulus orientation were arranged in complex repetitive patterns (Fig. 3*a*). Individual columns may be widely spaced or closely spaced and may be shaped isotropically or anisotropically, appearing as circular patches or as elongated bands (Fig. 3*b*). For every pattern, we calculated a 2D map of local column spacing and a 2D map of local column anisotropy, measuring the anisotropy of column shapes (large values for bandlike patterns, small values for patchy patterns). Based on these maps, we calculated four parameters describing the overall spatial organization of the OR patterns (Fig. 3*c*,*d*): (1) mean column spacing Λ, (2) SD σ_Λ of local column spacings across area 17 (spacing inhomogeneity), (3) mean bandedness α, and (4) SD σ_α of the local anisotropy parameter (shape inhomogeneity). Mean column spacing and bandedness measure whether a pattern predominantly contains large or small and bandlike or patchy OR columns, respectively; spacing inhomogeneity and shape inhomogeneity quantify pattern inhomogeneity across area 17.

Because an enhanced similarity among relatives can only be detected for parameters that exhibit considerable interindividual variability, we assessed the variability of these parameters across the population. As illustrated in Figure 4, all four parameters fulfill this requirement. Furthermore, patterns judged subjectively as similar exhibited similar parameter values. Figures 5 and 7 show examples of pairs of similar patterns of OR columns obtained from the two hemispheres of individual brains (Fig. 5) and from the brains of littermates (Fig. 7). Subjectively dissimilar patterns also exhibited substantially different parameter values (see Fig. 9). 2D maps of local column spacing and of local column anisotropy are displayed in Figure 6 for the patterns of OR columns obtained from the two hemispheres of individual brains in Figure 5 and in Figure 8 for the patterns from littermates shown in Figure 7. Although the patterns have similar average parameter values, their 2D parameter maps are not identical.

We subsequently compared the spacing and shape parameters of OR maps in the two hemispheres of 17 brains (Fig. 10*a–d*). Because the two hemispheres of a brain are genetically identical, genetically controlled features of visual cortical architecture are expected to be similar in the two brain hemispheres. Indeed, our data show similar parameter values in left and right areas 17. For mean column spacing, spacing inhomogeneity, and bandedness, the parameter values of left and right hemispheres displayed statistically significant correlations (Λ: $r = 0.78$, $p = 0.0002$; σ_Λ: $r = 0.49$, $p = 0.02$; α: $r = 0.46$, $p = 0.03$). The observed interhemispheric correlations are thus consistent with a substantial genetic influence on the developmental specification of visual cortical OR maps.

Alternatively, the similarity of measured parameters in left and right visual cortices may reflect the fact that the two hemispheres of one brain receive visual experiences that are typically more similar than the experiences of two different animals even if they are raised in the same environment. However, this ambiguity can be resolved if the parameter values are also significantly clustered

Table 2. Accuracy of estimation for the layout parameters mean column spacing (Λ), spacing inhomogeneity (σ_Λ), bandedness (α), and shape inhomogeneity (σ_α) using up to six 2-DG autoradiographs obtained from various cortical depths

parameter (P)	Range	Σ_{sec}	Σ_{hem}	ΔP	$\Delta P/\Sigma_{hem}$ (%)
Λ	1.0–1.4 mm	0.03 mm	0.094 mm	0.015 mm	16
σ_Λ	0.1–0.2 mm	0.026 mm	0.04 mm	0.013 mm	33
α	0.12–0.3	0.014	0.042	0.0071	17
σ_α	0.05–0.14	0.0086	0.019	0.0043	23

For all four parameters, the table lists the total range of interindividual variation (range), the average SD of parameter values calculated from sections at various cortical depths (Σ_{sec}), the SD of the section-averaged parameter values across different hemispheres (Σ_{hem}), the average SE (ΔP) of the section-averaged parameter values, and the relative error $\Delta P/\Sigma_{hem}$ as a percentage of the SD across hemispheres. Because 2-DG patterns obtained from different sections of the same cortex are much more similar to one another than patterns observed in different animals or in the two hemispheres of one brain, Σ_{sec} is substantially smaller than Σ_{hem}.

in littermates compared with unrelated animals. In Figure 10*e–h*, the values of the spacing and shape parameters of OR patterns from six litters are compared with one another and with the overall variability among all animals raised in the same environment as the littermates. In the littermates, the parameter values cluster, whereby the degree of clustering varies between litters and for different parameters (Fig. 10*e–h*). For instance, spacings in littermates typically differed by <80 μm, while they may differ

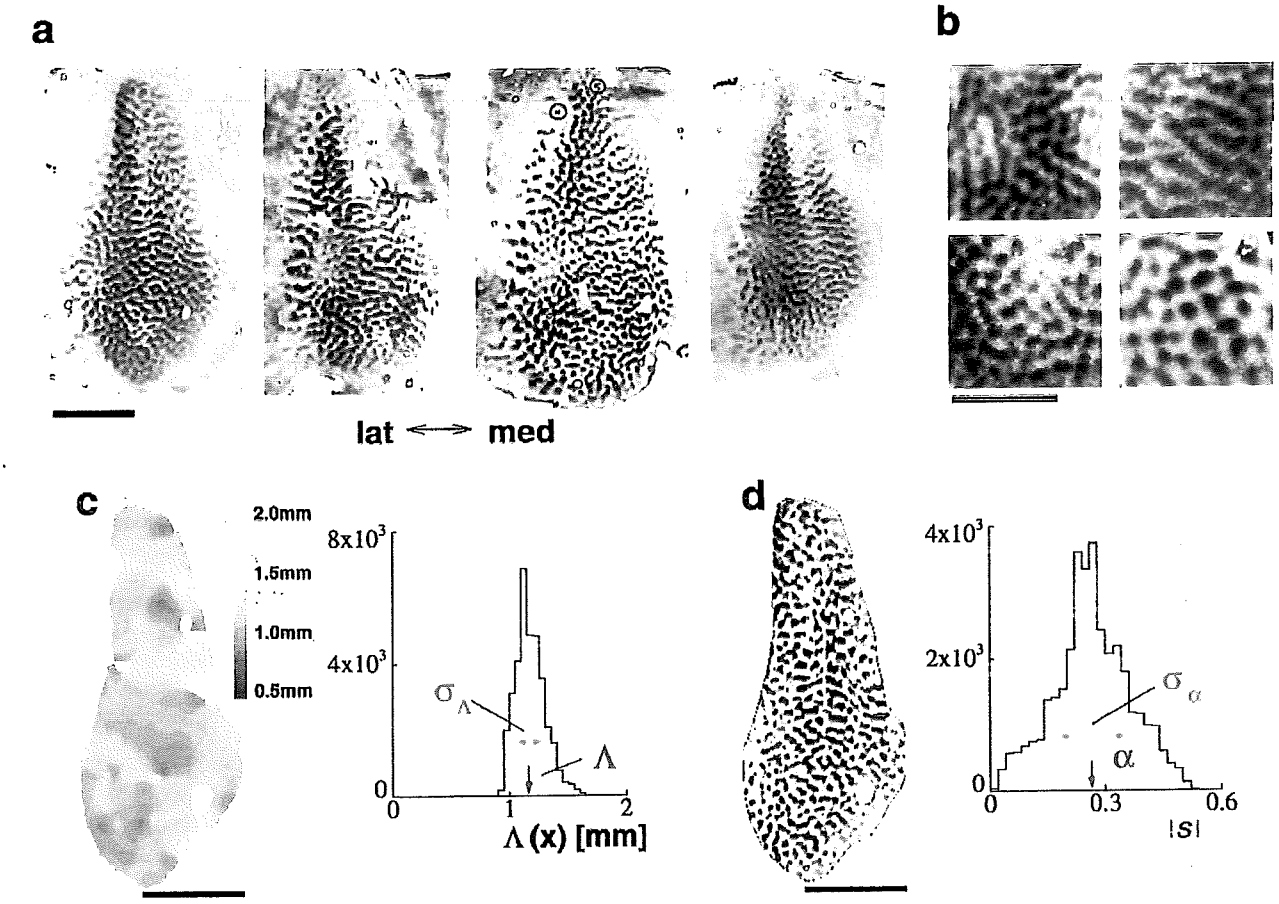

Figure 3. Layout properties of 2-DG-labeled OR domains in the primary visual cortex (area 17) of cats and their quantification. *a*, Representative examples from the analyzed data pool: 2-DG-labeled OR domains appear as *dark gray* to *black patches* or *stripes* on a *lighter gray background*. The 2-DG patterns were visualized on cortical flatmount sections and thus contain OR domains within the entire area 17. Anterior is at the *top* of each figure, and posterior is at the *bottom*. *lat*, Lateral; *med*, medial. *b*, Variability of pattern properties. OR domains vary in both the spacing of adjacent domains (*left column*, small; *right column*, large) and in the degree of anisotropy of domain shape (*top row*, band-like; *bottom row*, patchy). *c*, *d*, Quantitative analysis of the spacing (*c*) and shape (*d*) of OR columns. *c*, 2D map of local column spacing $\Lambda(x)$ (*left*) of a representative 2-DG pattern (left pattern in *a*) obtained by wavelet analysis, coded in *grayscale*: *light gray regions* exhibit larger-than-average spacing; *dark gray regions* exhibit smaller-than-average spacing. In the histogram of local column spacings (*right*), the mean column spacing Λ and the SD σ_Λ of local column spacings (spacing inhomogeneity) are marked by *red* and *blue arrows*, respectively. *d*, Local anisotropy parameter $s(x)$ *(yellow bars)* superimposed on the analyzed 2-DG pattern (*left*): The lengths of the *yellow bars* are proportional to the measure of local bandedness $|s(x)|$, with *long bars* indicating bandlike regions and *short bars* indicating patchy regions of the pattern. The *bars* are oriented perpendicular to the calculated local band orientation. The histogram of $|s(x)|$ (*right*) exhibits a broad peak with low and high values of $|s|$ corresponding to patchy and bandlike regions in the 2-DG pattern. The mean bandedness α and the SD σ_α of local bandedness (shape inhomogeneity) are marked by *red* and *blue arrows*, respectively. Scale bars: *a*, *c*, *d*, 10 mm; *b*, 5 mm.

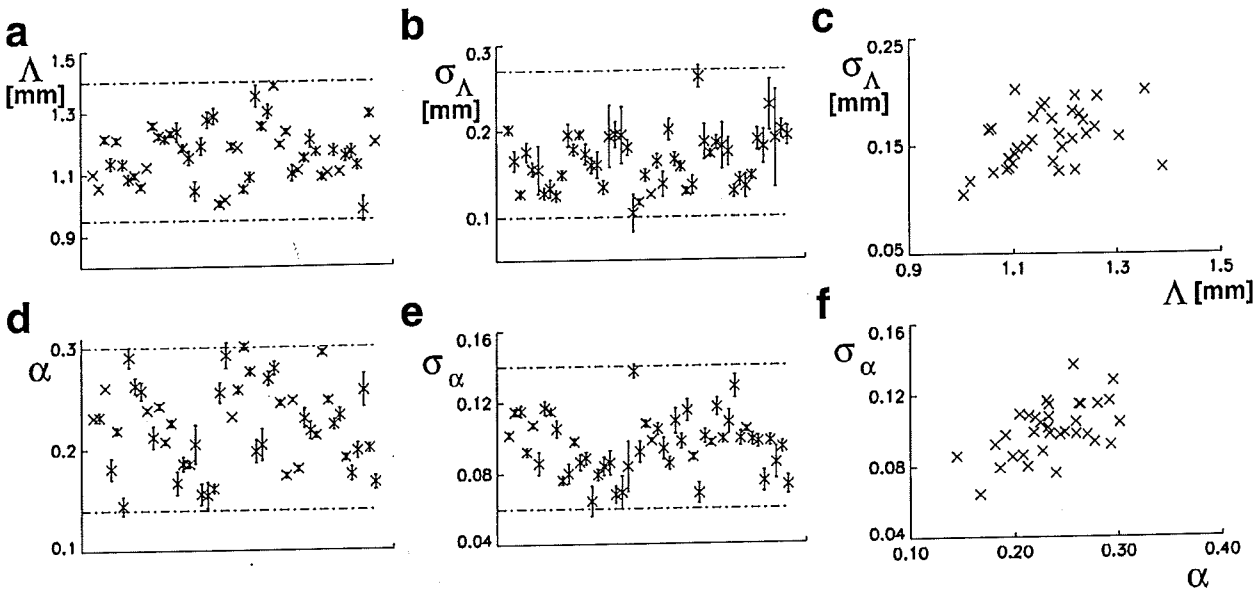

Figure 4. Interindividual variability (*a, b, d, e*) and relative independence (*c, f*) of the spacing and shape parameters mean spacing (Λ; *a*), spacing inhomogeneity (σ_Λ; *b*), bandedness (α; *d*), and shape inhomogeneity (σ_α; *e*) in 48 hemispheres from 31 animals. Values from individual hemispheres are indicated by ×s arranged along the *x*-axis in *a, b, d,* and *e*. Error bars show the SEM of the estimated parameter values. Scatter plots of the spacing and shape parameters are displayed in *c* and *f*. Note that the values of all four parameters display significant interindividual variability: Mean column spacings vary between 1.0 and 1.4 mm (*a*) and spacing inhomogeneities (σ_Λ) vary between 0.1 and 0.27 mm (*b*) in different animals. The shape parameters α and σ_α exhibit an even larger interindividual variability: Mean bandedness α varies by more than a factor of two between 0.14 for very patchy patterns and 0.3 for patterns largely composed of bands (*d*). Shape inhomogeneity varies between 0.06 and 0.14 (*e*). The *dashed–dotted lines* in *a, b, d,* and *e* mark the total range of interindividual variability.

by up to 400 μm in genetically unrelated animals. To test whether the observed degree of littermate clustering is sufficient to demonstrate a significant influence of genetic identity on the developmental specification of these parameters, we calculated the expected distributions of the ADLM of the parameter values assuming that parameters are statistically independent of the genetic identity of a hemisphere. To this end, the original data were randomized such that genetic relationships (I) among animals or (II) among all hemispheres were extinguished. For all four parameters, the actual ADLM values were smaller than the average value in randomized data, indicating littermate clustering (Fig. 10*i–l*). For mean column spacing, spacing inhomogeneity, and bandedness, littermate clustering was significant under both assumptions 1 and 2 (Fig. 10*i*, Λ: $P_I = 0.0046$, $P_{II} = 0.00014$; Fig.10*j*, σ_Λ: $P_I = 0.0028$, $P_{II} = 0.0005$; Fig.10k, α: $P_I = 0.035$; $P_{II} = 0.0023$).

To assess whether the observed littermate clustering of OR patterns may be caused by unspecific genetic factors controlling the animal's size or the size of its brain, we calculated the correlations of all spacing and shape parameters with the animal's weight and with the size of area 17. With the exception of a weak correlation of column spacing and area size ($r = 0.34$; $p = 0.03$), there were no significant correlations. There were also no significant correlations between the four parameters and the ages of the animals or the orientation of the visual stimuli. Our data therefore do not support the idea that unspecific genetic or experimental influences are responsible for the clustering of quantitative features of functional cortical architecture in littermates.

How does the observed substantial variability in the layout of visual cortical orientation columns affect visual information processing? Because of the retinotopic organization of area 17, each orientation hypercolumn processes information from a localized region of visual space. One might therefore imagine that the spatial resolution with which contour information is analyzed in area 17 is constrained by the total number of orientation hypercolumns in this area. This number, in turn, depends on column spacing and area size and can be estimated by the ratio of area size A and hypercolumn size Λ^2 (there is about one OR column per area Λ^2 of cortical surface). The size of area 17 varied between 330 and 575 mm^2, and the size of hypercolumns varied between 1.0 and 1.7 mm^2 in different hemispheres (Fig. 11*a*), demonstrating that both hypercolumn and area size exhibited pronounced interindividual variability with an approximately twofold range between smallest and largest values. Because hypercolumn and area size were only weakly correlated ($r = 0.34$; $p = 0.035$) (Fig. 11*a*), the total number of orientation hypercolumns also exhibited considerable interindividual variability, ranging between 240 and 410 in different animals (Fig. 11*b*). Thus cats exhibit smaller or larger orientation columns mostly regardless of whether they have a small or a large area 17. Considered individually, both hypercolumn and area size thus control considerable fractions of the interindividual variability of hypercolumn number (Fig. 11 *b,c*). Together, these observations indicate that genetic control of mean column spacing might effectively mediate a genetic influence on an animal's visual ability by controlling the number of visual cortical hypercolumns.

DISCUSSION

To our knowledge, our analysis represents the first study that correlates genetic similarity with quantitative features of functional cortical architecture. Although the similarity of columnar layouts in the two hemispheres of individual brains has been noted before for both monkey ocular dominance columns (Hor-

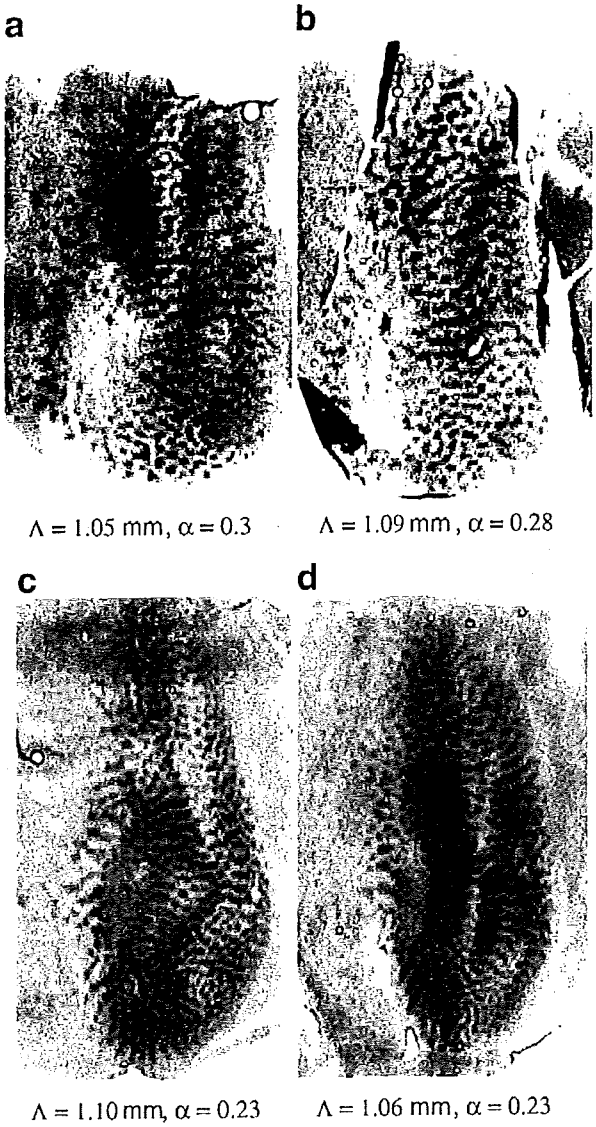

Figure 5. Examples of the similarity of patterns of 2-DG-labeled orientation columns in the two hemispheres of individual animals. The patterns of both the left (*a, c*) and right (*b, d*) hemispheres of cats C16 (*a, b*) and C1 (*c, d*) are displayed in a way so that the 17/18 border appears *left* in all *panels* (to this end, the right hemisphere patterns were mirror-inversed) to aid comparison. Note that the general appearance of the orientation column patterns (patchiness or bandedness of the pattern, spacing of adjacent domains, etc.) looks rather similar in the left and right hemispheres of both animals. Note furthermore that the quantified parameters (column spacing Λ and bandedness α) quantitatively reflect this similarity: Column spacing in the left and right area 17 of cat C16 was 1.05 and 1.09 mm, bandedness was 0.30 and 0.28, respectively. In cat C1, column spacings in the left and right area 17 were 1.10 and 1.06 mm; bandedness was 0.23 in both hemispheres. In the illustrated cases, column spacing Λ differed by only 40 μm in the left and right hemisphere of individual brains, whereas column spacing may differ by up to 400 μm among hemispheres from unrelated animals. Similarly, bandedness α differed by 0.02 at most in the illustrated hemisphere pairs, whereas this parameter may differ by up to 0.15 among hemispheres from unrelated animals.

ton and Hocking, 1996) and cat orientation and ocular dominance columns (Löwel et al., 1988), neither a detailed quantification of such observations in a large dataset nor an analysis of similarities and dissimilarities in genetically related and unrelated animals has been performed before. The present results are consistent with a substantial genetic influence on several parameters of visual cortical OR maps: mean spacing, spacing inhomogeneity, and mean bandedness were significantly more similar in the two hemispheres of individual brains and in related animals compared with the overall interindividual variability. The strong interindividual variability and the similarity of left and right visual cortical patterns observed here is comparable with the variability and left–right similarity exhibited by the overall size of representational areas in the primary somatosensory cortex (Riddle and Purves, 1995) and by functional modules in the olfactory bulb (Strotmann et al., 2000; Belluscio and Katz, 2001).

Epigenetic influences

Although it is conceivable in principle that the observed clustering of parameter values of visual cortical OR maps reflects an influence of shared nongenetic factors, this possibility appears rather unlikely if the developmental timetable for the formation of orientation columns is taken into account: axons from the lateral geniculate nucleus (LGN), providing visual input to visual cortical neurons, enter the cortex at about the time of birth (Ghosh and Shatz, 1992), when many cortical neurons are still migrating to their final positions (Luskin and Shatz, 1985). It is therefore unlikely that shared intrauterine environments of littermates can specifically influence the development of visual cortical OR maps. Furthermore, after birth, OR maps that exhibit all of the basic layout features found in adults form regardless of whether the animals have normal visual experience (Crair et al., 1998). Finally, although stripe rearing in early postnatal life increases the proportion of cells preferring the experienced orientation, major changes in OR map layout have not been observed (Blakemore and Cooper, 1970; Singer et al., 1981; Frégnac and Imbert, 1984; Sengpiel et al., 1999). Together, these studies indicate that shared experience is very unlikely to be responsible for the observed similarity of basic layout parameters of OR maps in genetically related animals.

Comparison with human twin studies

In the context of previous studies of the influence of genetic factors on morphometric features of the brain, the observation of significantly similar layouts of visual cortical orientation columns in related animals comes as a surprise. Although magnetic resonance imaging studies in humans demonstrated a substantial influence of genetic factors on "gross" morphometric brain measures such as intracranial volume, total gray or white matter volume (Baaré et al., 2001), and the overall volume of specifically chosen brain regions (Tramo et al., 1995, 1998; Pennington et al., 1999; Thompson et al., 2001), more specific features of brain morphology, such as sulcal patterns, were surprisingly different between monozygotic twins and thus did not exhibit a substantial genetic influence (Steinmetz et al., 1995; Bartley et al., 1997; Lohmann et al., 1999). These results suggested that the tightness of genetic control decreases from gross- to fine-grained features of cortical architecture. However, our present data quantitatively demonstrate that fine-grained and functionally relevant aspects of neocortical organization can also be influenced to a significant degree by genetic information.

Experience dependence

The demonstration of a significant genetic influence on quantitative features of visual cortical organization has important implications for the study of the impact of experience on cortical organization. Previously, analyses of the effects of visual experi-

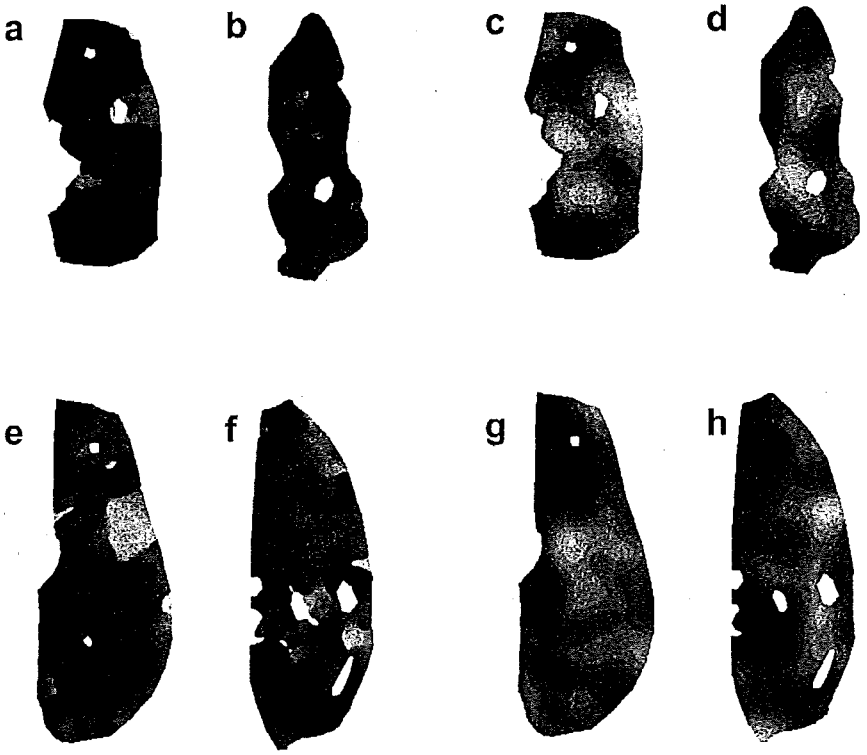

Figure 6. 2D maps of local column spacing (*a*, *b*, *e*, *f*) and local bandedness (*c*, *d*, *g*, *h*) for the patterns obtained from left–right pairs of hemispheres displayed in Figure 5. The maps are arranged as in Figure 5: the maps in *a* and *c* were derived from the pattern in Figure 5*a*, the maps in *b* and *d* were derived from the pattern in Figure 5*b*, the maps in *e* and *g* were derived from the pattern in Figure 5*c*, and the maps in *f* and *h* were derived from the pattern in Figure 5*d*.

ence on column layout in the visual cortex have largely ignored the animals' genetic backgrounds. Thus, in the light of our present findings, genetically induced variability may have been interpreted as evidence for experience dependence in previous studies. For instance, if the spacing of ocular dominance patterns is subject to a similar degree of genetic influence as that of orientation columns, the observation of Löwel (1994) and Tieman and Tumosa (1997) that animals raised with strabismus or alternating monocular exposure exhibit an increased spacing of ocular dominance columns might have been confounded by a genetic dissimilarity between experimental and control groups. In general, the occurrence of a pronounced interindividual variability together with a substantial genetic influence on visual cortical organization emphasize that to obtain unambiguous results with respect to the impact of experience on cortical organization, experimental and control groups must be composed of littermates.

Mechanisms of genetic control

The similarity of quantitative parameters of visual cortical OR maps in littermates strongly suggests the existence of developmental mechanisms that mediate a genetic influence on the layout of functional cortical maps. However, the available evidence is insufficient to determine the precise nature of these mechanisms. Notably, conceivable mechanisms differ considerably in how directly genetic information might control visual cortical architecture. The most extreme possibility that appears consistent with the available data is the direct genetic prespecification of the orientation preferences of individual visual cortical neurons by some kind of (to be identified) molecular recognition mechanisms. Obviously, such a model can explain our results. Nevertheless, the observed littermate clustering can be explained just as well by genetic influences on mechanisms for the activity-dependent selection of cortical circuitry (see below). To identify the precise mechanism of genetic control, it will be important for future studies to further characterize the strength and nature of genetic influences on cortical functional maps. For instance, the hypothesis of genetic prespecification in detail predicts that maps in genetically identical animals such as clones or identical twins should resemble each other in every detail. Consequently, this hypothesis would be falsified if maps in such animals exhibit similar parameters, which is predicted by our results, but differ in the exact arrangement of the columns. More generally, however, the comparison of maps in genetically identical animals is a priori incapable of identifying the mechanisms by which genetic information influences functional cortical maps (for a detailed discussion, see Miller et al., 1999). Instead, genuinely new paradigms will be needed to identify with certainty the mechanisms mediating the genetic control of functional cortical maps (see Specific versus unspecific genetic factors).

Thus, while our results are in line with recent experiments on visual cortical development indicating that the initial development of cortical maps is largely independent of visual experience (Gödecke and Bonhoeffer, 1996; Crair et al., 1998; Löwel et al., 1998; Crowley and Katz, 2000), it is important to note that they are also fully consistent with the hypothesis that the functional architecture of the visual cortex essentially develops through activity-dependent mechanisms (Stryker, 1991; Goodman and Shatz, 1993). Theoretical studies have demonstrated that even if cortical columns develop exclusively through a self-organization process driven by individual experience, genetic information may determine the final pattern layout by controlling cellular parameters or boundary and initial conditions (Gierer, 1988, Wolf et al., 1996; Miller et al., 1999). Various mathematical models for the activity-dependent formation of column patterns predict that the spacing of adjacent columns is determined by cellular parameters such as the width of dendritic or axonal arborizations (Miller, 1995; Swindale, 1996). Shape features of column patterns are

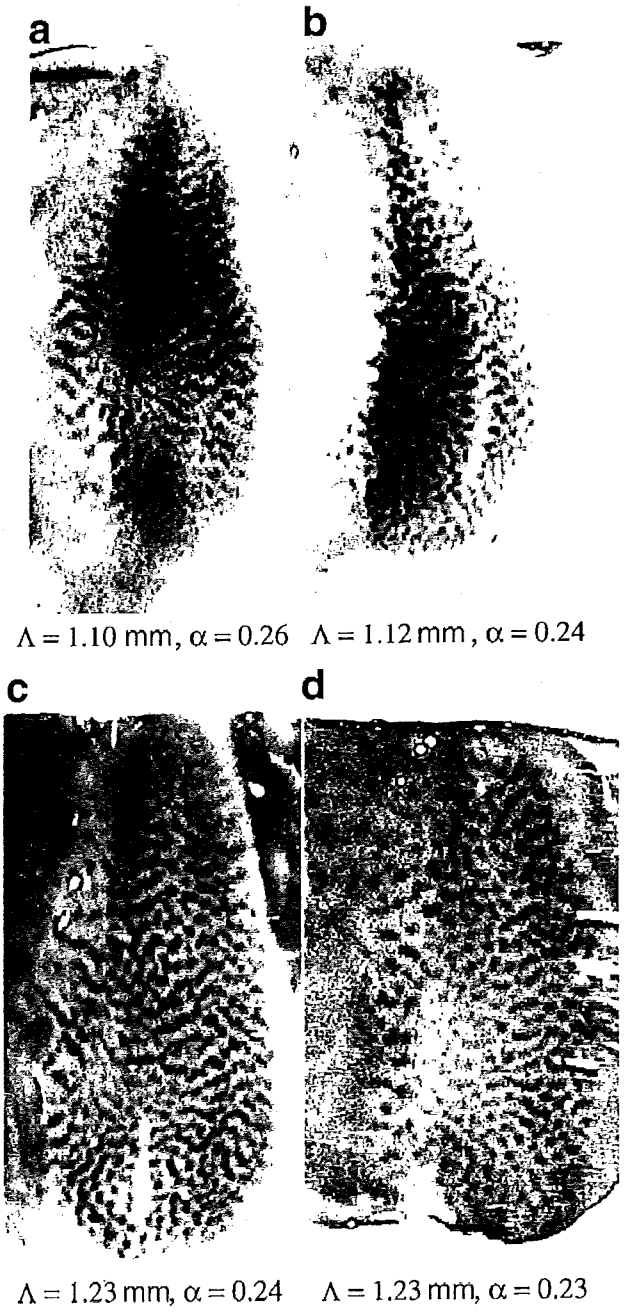

Figure 7. Examples of the similarity of patterns of 2-DG-labeled orientation columns in littermates. The orientation column patterns of the related cats C4 and C5 (*a*, *b*) and C6 and C7 (*c*, *d*) are displayed such that the 17/18 border appears *left* in all *panels*. Note that the general appearance of the orientation column patterns (patchiness or bandedness of the pattern, spacing of adjacent domains, etc.) is rather similar in the littermates. Note furthermore that the quantified parameters (column spacing Λ and bandedness α) quantitatively reflect this similarity: Column spacing in the right area 17 of cats C4 and C5 was 1.10 and 1.12 mm, and bandedness was 0.26 and 0.24, respectively. In the littermate cats C6 and C7, column spacings in the right area 17 were 1.23 mm for both animals, and bandedness was 0.24 and 0.23, respectively. As for pairs of left and right hemispheres from individual animals (Fig. 5), the differences in parameter values in littermates are very small compared with the overall interindividual variability (compare Fig. 4).

influenced by similar parameters (Wolf and Geisel, 1998, 2000). Genetic determination of the parameters of an activity-dependent developmental process is therefore sufficient to explain the observed littermate clustering and left/right brain similarities.

In addition, it should be noted that our results do not imply that column patterns in left–right hemisphere pairs or in littermates are more or less identical or have identical parameter values. In fact, one would expect even left–right hemisphere pairs that are genetically identical to exhibit different parameter values, because identical parameter values can only result if genetic information is expressed absolutely symmetrically in the two hemispheres and nongenetic factors (such as random events in development) do not play any role. Consistent with this prediction, we indeed find that some of the parameters of left and right brain hemispheres differ by more than two estimated SEs and are therefore presumably significantly different.

Specific versus unspecific genetic factors

Although the precise mechanism underlying the observed littermate clustering of orientation column layout is unknown, our data suggest that genetic factors control at least a considerable fraction of the variability of visual cortical columnar architecture. These genetic factors may either specifically affect the layout of visual cortical columns (and nothing else) or unspecifically influence a variety of features of brain organization including column layout. Because we did not observe strong correlations between the quantified layout properties and body weight or the size of area 17, our data indicate that the observed littermate clustering is not caused by factors unspecifically affecting growth processes throughout the body or the brain. In particular, because there was only a weak correlation between column size and area size, our data demonstrate that the total number of orientation columns is controlled by more than one factor. However, it is very possible that other unspecific factors do play a role in orientation column layout. For instance, it is conceivable that genetic factors affecting cellular parameters such as the radius of dendritic or axonal arborizations contribute to the similarity of orientation columns in area 17 of littermates. Another possibility is raised by theoretical studies that demonstrated that in mathematical models of the activity-dependent development of column patterns, the correlational structure of activity patterns in the LGN affects the spacing of columns (Goodhill, 1993; Scherf et al., 1999; Wolf et al., 2000). Therefore, these models predict that every factor that affects the structure of correlations within the LGN may also affect the spacing of columns in the visual cortex. Candidate factors include the number of retinal ganglion cells, the time of eye opening, and the synaptic organization of LGN circuitry. To identify the relevant factors, future studies will have to analyze how the variability of functional cortical architecture correlates with a wide variety of properties at the cellular, circuit, and systems level.

Genetic control of visual abilities

Our observation that the total number of orientation hypercolumns in area 17 exhibits a large degree of interindividual variability raises the question of whether genetic control of cortical columnar architecture mediates a genetic influence on an animal's visual abilities. In this context, it is interesting to note that tracing

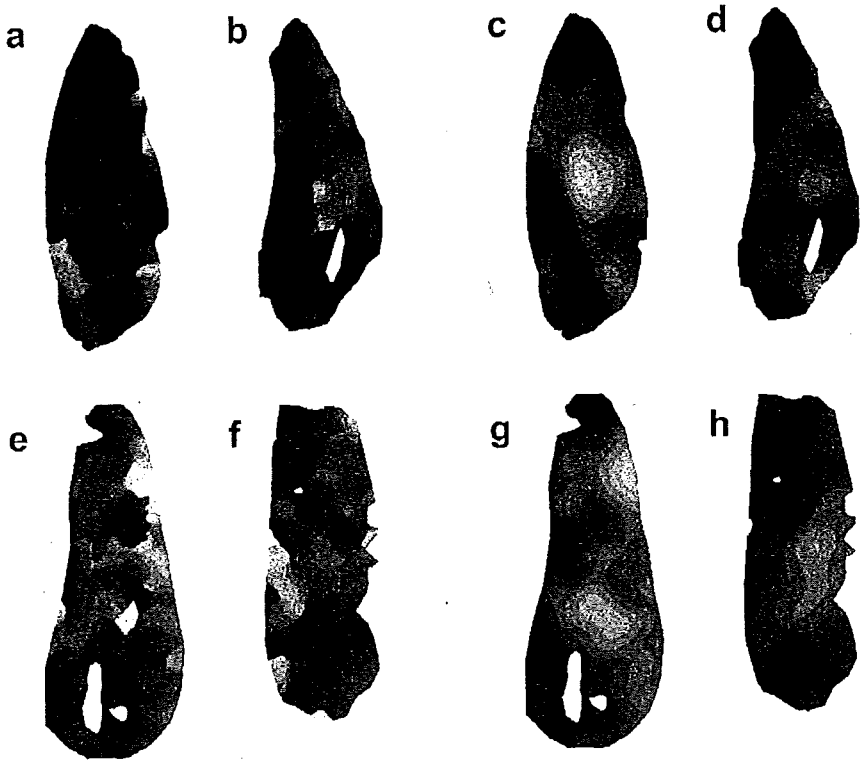

Figure 8. 2D maps of local column spacing (*a, b, e, f*) and local bandedness (*e, d, g, h*) for the patterns in littermates displayed in Figure 7. The maps are arranged as in Figure 7: the maps in *a* and *c* were derived from the pattern in figure 7*a*, the maps in *b* and *d* were derived from the pattern in Figure 7*b*, the maps in *e* and *g* were derived from the pattern in Figure 7*c*, and the maps in *f* and *h* were derived from the pattern in Figure 7*d*.

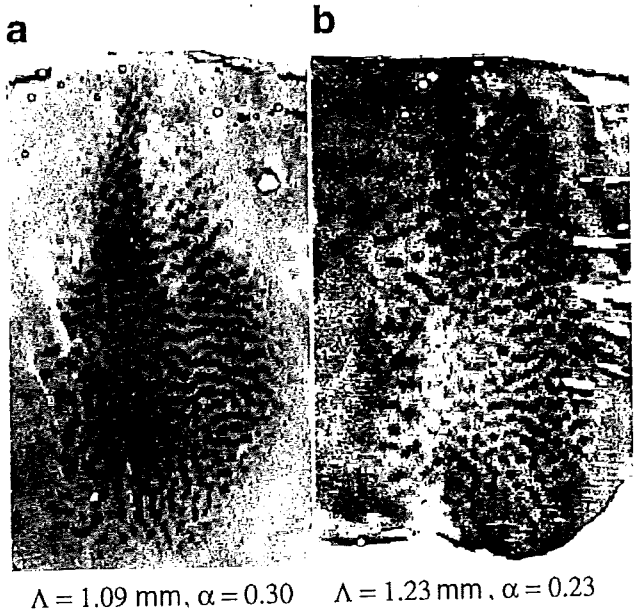

Figure 9. Examples of the dissimilarity of orientation column patterns in unrelated cats (cats C24 and C7). Arrangement of the patterns is as in Figures 5 and 7. Column spacing in the two cats was 1.09 and 1.23 mm, respectively; anisotropy was 0.30 and 0.23, respectively, indicating very dissimilar patterns (compare with Figs. 5 and 7).

experiments in the human temporal cortex have shown that the left hemisphere specialization for language processing is accompanied by a larger number of distinct cortical modules in the posterior part of Brodmann area 22 (Galuske et al., 2000).

These results suggest that the number of functional cortical units might indeed be related to the processing capabilities of an area. In the visual cortex, one can easily imagine that the total number of orientation hypercolumns directly affects visual function. Each orientation hypercolumn analyzes contour information from a small region of visual space. With a larger number of orientation hypercolumns, contour information can be independently assessed for more and finer-grained regions of visual space, which might improve the capacity of the visual system for the processing of complex images. In other words, a larger number of orientation hypercolumns would lead to a better "coverage" of contour orientation and retinotopic position by the cortical map (Swindale et al., 2000). If visual performance is indeed affected by the total number of orientation hypercolumns in area 17, then our results would predict a substantial degree of interindividual variability in those abilities that are mediated by visual cortical architecture. In this case, genetic control of mean column spacing could easily mediate a genetic influence on an animal's visual ability by controlling the number of hypercolumns. At present, however, this possibility cannot be assessed, because virtually nothing is known about the degree of interindividual variability in visual abilities that are mediated by visual cortical circuitry or about their genetic control.

The behavioral genetics of human cognitive abilities has for decades pointed to a prominent influence of genetic factors on cognitive performance (Bouchard, 1998) and accordingly on the underlying aspects of brain organization (Thompson et al., 2001). However, the developmental processes through which genetic information can influence cortical structure and function, and thereby an individual's sensory, motor, and cognitive abilities, have remained essentially unknown to date. Our results suggest that quantitative features of neocortical architecture such as size

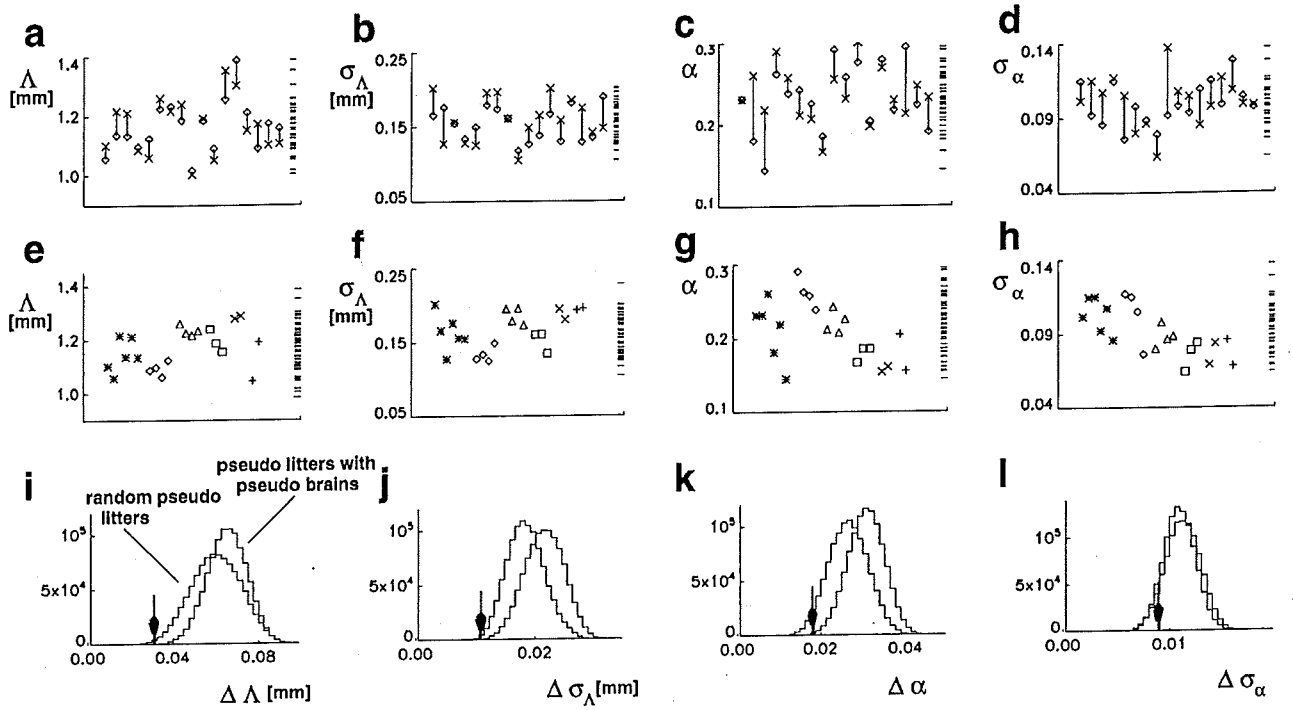

Figure 10. Clustering of parameter values in left and right hemispheres and among littermates. *a, e, i,* Mean column spacing Λ. *b, f, j,* Spacing inhomogeneity σ_Λ. *c, g, k,* Bandedness α. *d, h, l,* Shape inhomogeneity σ_α. *a–d,* Comparison of the parameter values in the left and right visual cortices of 17 animals. Left and right hemisphere values are marked by ×s and ◇s, respectively. For comparison, the distributions of parameter values from all hemispheres are plotted on the *right side* of the figures (*horizontal lines*). Note that values in the left and right hemispheres are often rather similar and that significant correlations were found for mean column spacing, spacing inhomogeneity, and bandedness, but not for shape inhomogeneity ($r = 0.17$; $p = 0.26$). In addition, there were no systematic differences in the architecture of left and right area 17 (i.e., no signs of lateralization for the measured parameter set) ($p > 0.15$; permutation test for the average sign of left–right differences). *e–h,* Littermate clustering: Comparison of the parameter values in six litters. Data points from littermates are marked by identical symbols (*, ◇, △, □, ×, and + from *left* to *right*). For comparison, the distributions of parameter values from all hemispheres of animals raised in the same environment are plotted on the *right side* of the figures (*horizontal lines*). Note that values from littermates cluster, whereby the degree of clustering varies between litters and for different parameters. *i–l,* Permutation tests for genetic influences on quantified parameters of visual cortical OR maps. Analysis of 6×10^6 randomly generated pseudolitters demonstrates statistically significant littermate clustering for mean column spacing (*i*), spacing inhomogeneity (*j*), and bandedness (*k*): It is highly unlikely to observe the ADLMs $\Delta\Lambda$ (*i*), $\Delta\sigma_\Lambda$ (*j*) and $\Delta\alpha$ (*k*) of real litters (*arrows*) by chance if no genetic component is present. Littermate clustering observed for shape inhomogeneity σ_α (*l*) is, however, not statistically significant in our data set (*l*: $P_I = 0.092$; $P_{II} = 0.083$). The ADLM values calculated for the real litters are compared with two distributions obtained by either (I) assigning animals raised in the same environment to random pseudolitters (*left histograms*; see *i* or (II) first forming pseudobrains of randomly chosen hemispheres, which were then assigned to pseudolitters (*right histograms*; see *i*). If correlations of left and right hemisphere parameter values are of entirely epigenetic origin, randomization scheme I applies and extinguishes all genetic influences. However, if these correlations are of genetic origin, randomization scheme II extinguishes all genetic influences by generating pseudobrains with uncorrelated parameter values in the left and right hemispheres. For all four parameters, the real ADLMs are smaller than the large majority of ADLMs calculated from randomized data.

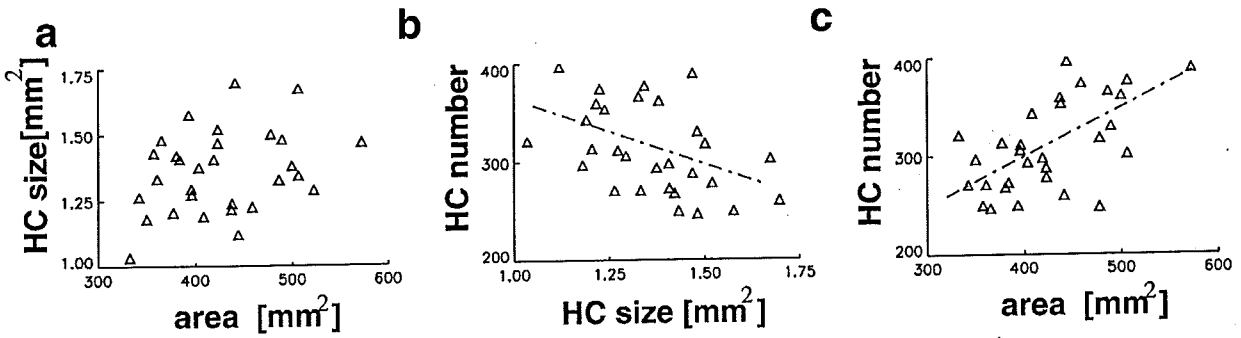

Figure 11. The total number of orientation hypercolumns (*HCs*) in cat area 17 is determined by the column spacing Λ and the area size *A*. *a,* Scatter plot of HC size Λ^2 versus area size *A*. Note that there is only a weak correlation of HC size and area size ($r = 0.34$; $p = 0.035$), indicating that larger areas 17 do not necessarily contain larger HCs. *b, c,* Scatter plots of the total number of HCs in area 17 (A/Λ^2) versus HC size (*b*) ($r = -0.51$; $p = 0.001$) and versus area size (*c*) ($r = 0.63$; $p = 0.0001$). *Dash-dotted lines* are regression lines. Note that both HC size and area size explain substantial fractions of the interindividual variability in HC number (Λ^2, 26%; *A*, 39%), indicating that, on average, large areas 17 and areas 17 with small HCs contain more modules.

and shape of cortical modules may be key targets of genetic control.

REFERENCES

Baaré WFC, Pol HEH, Boomsma DI, Posthuma D, de Geus EJC, Schnack HG, van Haren NEM, van Oel CJ, Kahn RS (2001) Quantitative genetic modeling of variation in human brain morphology. Cereb Cortex 11:816–824.

Bartley AJ, Jones DW, Weinberger DR (1997) Genetic variability of human brain size and cortical gyral patterns. Brain 120:257–269.

Blakemore C, Cooper GF (1970) Development of the brain depends on the visual environment. Nature 228:477–478.

Belluscio L, Katz LC (2001) Symmetry, stereotypy, and topography of odorant representations in mouse olfactory bulbs. J Neurosci 21: 2113–2122.

Bouchard TJ (1998) Genetic and environmental influences on adult intelligence and special mental abilities. Hum Biol 70:257–279.

Crair MC, Gillespie DC, Stryker MP (1998) The role of visual experience in the development of columns in cat visual cortex. Science 279:566–570.

Creutzfeldt OD (1995) Cortex cerebri: performance, structural and functional organization of the cortex. Oxford: Oxford UP.

Crowley JC, Katz LC (2000) Early emergence of ocular dominance columns. Science 290:1321–1324.

Farge M (1992) Wavelet transforms and their application to turbulence. Annu Rev Fluid Mech 24:392–457.

Frégnac Y, Imbert M (1984) Development of neuronal selectivity in primary visual cortex of cat. Physiol Rev 64:325–434.

Galuske RAW, Schlote W, Bratzke H, Singer W (2000) Interhemispheric asymmetries of the modular structure in human temporal cortex. Science 289:1946–1949.

Ghosh A, Shatz CJ (1992) Pathfinding and target selection by developing geniculocortical axons. J Neurosci 12:2811–2822.

Gierer A (1988) Spatial organization and genetic information in brain development. Biol Cybern 59:13–32.

Gödecke I, Bonhoeffer T (1996) Development of identical orientation maps for two eyes without common visual experience. Nature 379:251–254.

Goodhill GJ (1993) Topography and ocular dominance: a model exploring positive correlations. Biol Cybern 69:109–118.

Goodman CS, Shatz CJ (1993) Developmental mechanisms that generate precise patterns of neuronal connectivity. Cell 72:77–98.

Horton JC, Hocking DR (1996) Intrinsic variability of ocular dominance column periodicity in normal macaque monkeys. J Neurosci 16:7228–7339.

Hubel DH, Wiesel TN (1962) Receptive fields, binocular interaction, and functional architecture in cat's visual cortex. J Physiol (Lond) 160:215– 243.

Kaschube M, Wolf F, Geisel T, Löwel S (2000) Quantifying the variability of patterns of orientation columns in the visual cortex of cats. Neurocomputing 32–33:415–423.

LeVay S, Nelson SB (1991) Columnar organization of the visual cortex. In: Vision and visual dysfunction (Cronly-Dillon JR, ed), pp 266–315. Houndmill, UK Macmillan.

Lohmann G, von Cramon DY, Steinmetz H (1999) Sulcal variability of twins. Cereb Cortex 9:754–763.

Löwel S (1994) Ocular dominance column development: strabismus changes the spacing of adjacent columns in cat visual cortex. J Neurosci 14:7451–7468.

Löwel S, Singer W (1990) Tangential intracortical pathways and the development of iso-orientation bands in cat striate cortex. Brain Res Dev Brain Res 56:99–116.

Löwel S, Freeman B, Singer W (1987) Topographic organization of the orientation column system in large flat-mounts of the cat visual cortex: a 2-deoxyglucose study. J Comp Neurol 255:401–415.

Löwel S, Bischof H-J, Leutenecker B, Singer W (1988) Topographic relations between ocular dominance and orientation columns in the cat striate cortex. Exp Brain Res 71:33–46.

Löwel S, Schmidt KE, Kim D-S, Wolf F, Hoffsümmer F, Singer W, Bonhoeffer T (1998) The layout of orientation and ocular dominance domains in area 17 of strabismic cats. Eur J Neurosci 10:2629– 2643.

Luskin MB, Shatz CJ (1985) Neurogenesis of the cat's primary visual cortex. J Comp Neurol 242:611–631.

Miller KD (1995) Receptive fields and maps in the visual cortex: models of ocular dominance and orientation columns. In: Models of neural networks III (Domany E, van Hemmen LJ, Schulten K, eds), pp 55–78, New York: Springer-Verlag.

Miller KD, Erwin E, Kayser A (1999) Is the development of orientation selectivity instructed by activity? J Neurobiol 41:44–57.

Pennington BF, Filipek PA, Lefly D, Chahabildas N, Kennedy DN, Simon JH, Filley CF, Galaburda A, DeFries JC (1999) A twin study of size variations in the human brain. J Cogn Neurosci 12:223–232.

Price D, Willshaw DJ (2000) Mechanisms of cortical development. Oxford: Oxford UP.

Recanzone G (2000) Cerebral cortex plasticity: perception and skill acquisition. In: The new cognitive neurosciences (Gazzaniga MS, ed), pp 237–250. Boston: MIT.

Riddle DR, Purves D (1995) Individual variation and lateral asymmetry of the rat primary somatosensory cortex. J. Neurosci. 15:4184– 4195.

Scherf O, Pawelzik K, Wolf F, Geisel T (1999) Theory of ocular dominance pattern formation. Phys Rev E Stat Phys Plasmas Fluids Relat Interdiscip Topics 59:6977–6993.

Sengpiel F, Stawinsky P, Bonhoeffer T (1999) Influence of experience on orientation maps in cat visual cortex. Nat Neurosci 2:727–732.

Singer W (1995) Development and plasticity of cortical processing architectures. Science 270:758–764.

Singer W, Freeman B, Rauschecker J (1981) Restriction of visual experience to a single orientation affects the organization of orientation columns in cat visual cortex: a study with deoxyglucose. Exp Brain Res 41:199–215.

Somogyi P, Tamás G, Lujan R, Buhl EH (1998) Salient features of synaptic organization in the cerebral cortex. Brain Res Brain Res Rev 26:113–135.

Steinmetz H, Herzog A, Schlaug G, Huang Y, Jancke L (1995) Brain (a)symmetry in monozygotic twins. Cereb Cortex 5:296–300.

Strotmann J, Conzelmann S, Beck A, Feinstein P, Breer H, Mombaerts P (2000) Local permutations in the glomerular array of the mouse olfactory bulb. J Neurosci 20:6927–6938.

Stryker MP (1991) Activity-dependent reorganization of afferents in the developing mammalian visual system. In: Development of the visual system (Lam DM, Shatz CJ, eds), pp 267–287. Cambridge, MA: MIT.

Swindale NV (1996) The development of topography in the visual cortex: a review of models. Network 7:161–247.

Swindale NV, Shoham D, Grinvald A, Bonhoeffer T, Hubener M (2000) Visual cortex maps are optimized for uniform coverage. Nat Neurosci 3:822–826.

Thompson PM, Cannon TD, Narr KL, van Erp T, Poutanen V-P, Huttunen M, Lönnqvist J, Standertskjöld-Nordenstam C-G, Kaprio J,Khaledy M, Dail R, Zoumalan CI, Toga AW (2001) Genetic influences on brain structure. Nat Neurosci 4:1253–1258.

Tieman SB, Tumosa N (1997) Alternating monocular exposure increases the spacing of ocularity domains in area 17 of cats. Vis Neu-rosci 14:929–938.

Tramo MJ, Loftus WC, Thomas CE, Gazzaniga MS (1995) Surface area of human cerebral cortex and its gross morphological subdivisions: *in vivo* measurements in monozygotic twins suggest differential hemisphere effects of genetic factors. J Cogn Neurosci 7:292–301.

Tramo MJ, Loftus WC, Stukel TA, Green RL, Weaver JB, Gazzaniga MS (1998) Brain size, head size, and intelligence quotient in monozygotic twins. Neurology 50:1246–1252.

Weliky M, Katz LC (1999) Correlational structure of spontaneous activity in the developing lateral geniculate nucleus in vivo. Science 285:599–604.

Wolf F, Geisel T (1998) Spontaneous pinwheel annihilation during visual development. Nature 395:73–78.

Wolf F, Geisel T (2000) A general theory of pinwheel stability. Soc Neurosci Abstr 26:1472.

Wolf F, Bauer H-U, Pawelzik K, Geisel T (1996) Organization of the visual cortex. Nature 382:306–307.

Wolf F, Pawelzik K, Scherf O, Geisel T, Löwel S (2000) How can squint change the spacing of ocular dominance columns? J Physiol (Paris) 94:525–537.